Available online at www.sciencedirect.com

ScienceDirect

Procedia Chemistry 17 (2015) 9 – 15

Procedia Chemistry

3rd International Seminar on Chemistry 2014

Computational study of structure and stability of polymeric complexes of $[Fe_4(Htrz)_8(trz)_4]^{4+}$ and $[Fe_4(Htrz)_{12}]^{8+}$

Asep Wahyu Nugraha[a,b], Djulia Onggo[c], Muhamad A Martoprawiro[c,*]

[a]*Physical Chemistry Research Group, Faculty of Mathematics and Natural Sciences Universitas Negeri Medan, Willem Iskandar V Medan Estate Medan 20222, Medan, Indonesia*

[b]*Doctoral Program in Chemistry, Faculty of Mathematics and Natural Sciences, Institut Teknologi Bandung, Jl. Ganesha 10 Bandung, 40132*

[c]*Inorganic and Physical Chemistry Research Division, Faculty of Mathematics and Natural Sciences, Institut Teknologi Bandung, Jl. Ganesha 10 Bandung 40132*

Abstract

The computational study of iron(II) 1,2,4-4Htriazole complexes was performed to determine structure and stability of $[Fe_4(Htrz)_8(trz)_4]^{4+}$and $[Fe_4(Htrz)_{12}]^{8+}$ complexes. The computations utilized HartreeFock (HF) and Density Functional Theory (DFT) with UHF, B3LYP, and TPSSh methods and 3-21G, 6-31G(d), and TZVP basis sets. The calculation resulted in the predicted structure of $[Fe_4(Htrz)_8(trz)_4]^{4+}$ and $[Fe_4(Htrz)_{12}]^{8+}$ polymeric complexes. No experimental data are available for these structure, however, the predicted structures are similar to Cu(II) complexes. The energy difference using TPSSh and TZVP for $[Fe_4(Htrz)_8(trz)_4]^{4+}$complex was -9285.974 kJ/mole and for $[Fe_4(Htrz)_{12}]^{8+}$ complex was -3501.534 kJ/mole. The deprotonated complexes of iron(II) 1,2,4-4H triazole are predicted more stable than the protonated ones.

Keywords: computational study, 1,2,4-4H-triazole, iron(II), stability, structure

1. Introduction

A spin transition (ST) material is a material with two properties, that is, it is capable of displaying two different magnetic properties with any specific external disturbances. Those external disturbances that may result in the changes are, among others, change in temperature, change in pressure, light induction, and polymer formation[1,2,3,4]. Material with the ST features can be used for various applications such as switches or sensors caused by light, temperature, pressure, and other physical treatments. In addition, the compounds with TS features can also be used for a data storage requirement, so that data storage can use materials in molecular scales[5,6]. One of the complexes with the ST properties is a complex formed between iron(II) with 1,2,4-4H-triazole ligand. Experimental observations have disclosed that iron(II) with a 1,2,4-4H-triazole ligand complex in low spin condition is lilac in color and diamagnetic, whereas when the temperature is raised, this complex is colorless and paramagnetic. This

* Corresponding author. Tel.: +62-81221222424; fax: +62-22-2504154
E-mail address: muhamad@chem.itb.ac.id

Peer-review under responsibility of Department of Chemistry, Faculty of Mathematics and Natural Sciences, Padjadjaran University
doi:10.1016/j.proche.2015.12.107

change in property occurs reversibly at around room temperature and is also affected by the types of anion and the number of water molecules.

The previous experiments[7,8] showed that one of the 1,2,4-4H-triazole ligands is deprotonated, so that a complex with structure of$[Fe_4(Htrz)_8(trz)_4]^{4+}$ was obtained. Meanwhile, another experiment demonstrated that there was no deprotonated ligand, so they obtained a complex with a structure of $[Fe_4(Htrz)_{12}]^{8+}$ [9]. A computational study of deprotonated complexes, especially for the Fe(II) 1,2,4-4H-triazole complex, has not been conducted by previous researchers.

This study is to determine the amount of energy differences computationally for the formation of $[Fe_4(Htrz)_8(trz)_4]^{4+}$ and $[Fe_4(Htrz)_{12}]^{8+}$ complexes and to compare complex stability of both structures. Due to unavailability of experimental structure of these complexes, the geometry estimate from the structure of copper(II) complex of triazole. Based on XRD measurement, the complex compound formed from copper(II) ion with 1,2,4-4H-triazole is polymeric with triazole ligand as its bridge. Since the single-crystal structure of the $[Fe(Htrz)_2trz]^+$ complex has not been successfully determined previously, then the Cu(II) complex of triazole was made as a model for geometry optimization of Fe-triazole structures.

2. Theoretical Study

Sugiyarto et al. (1994)[7], studied $Fe(Htrz)_2(trz)X$ complex (X = BF_4^-, ClO_4^- and PF_6^-) experimentally by observing magnetization and the Mossbauer's spectra. Their experimental results showed that the Fe(II) triazol complex and BF_4^- and ClO_4^- anions have a transition temperature above room temperature, whereas for the PF_6^- anion under room temperature (Kahn et al., 1998). Lavrenova et al. (2003)[9], demonstrated the presence of hydrate on the $[Fe(Htrz)_3]Cl_2$ complex that would decrease its transition temperature to the lower one. However, Faulmann et al. (2011)[8], showed that the nano size complex of $[Fe(Htrz)_2(trz)](BF_4)$ by using a silicate matrix has the transition temperature above 100°C. Dirtu et al. (2010)[10], also showed the pattern similarity between $[Fe(NH_2trz]_3(NO_3)_2$ and $[Cu(NH_2trz)_3](NO_3)_2.H_2O$ structures determined by SEM and X-ray powder diffraction. These structures may be used to estimate $[Fe(Htrz)_2(trz)BF_4$ (Htrz = 1,2,4-H4-triazole, trz^{-1} = 1,2,4-triazolato) structures in low spin (LS) and high spin (HS) conditions.

Previous experiment[11], showed that the complex formed a polymer in which the 1,2,4-4H-triazole ligand act as a bridge between Fe(II) ions as illustrated in Figure. 1. With the usage of visualization of geometry optimization results it is drawn the iron(II) 1,2,4-4H-triazole complex structure that also play as comparator of experimental results.

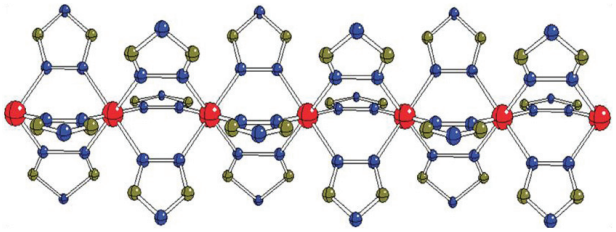

Fig. 1. The iron(II) polymer crystal and 1,2,4-4H-triazole ligand structures

Using the DFT means of the properties from energetic, molecules geometries, and the molecular interactions. The Hohenberg-Kohn theory and the other theory of DFT provide the knowledge and determination some problem in the physic and chemistry[12]. In relation with the TPSS method (Tao, Perdew, Staroverov, and Scuseria) as revision of the PKZB's (Perdew, Kurth, Zupan, and Blaha) approach and the MGGA (meta-GGA) functional stabilizer has been discussed[13]. The variable section of the TPSS functional has a general form of a gradient-enhanced LSDA exchange, as it is illustrated in equation 1.

$$E_x^{TPSS}[\rho_\alpha, \rho_\beta] = \sum_{\sigma=\alpha,\beta} \int \rho_\sigma \epsilon_x^{LSDA}(\rho_\sigma)\, F_x(\rho_\sigma, \nabla\rho_\sigma, \tau_\sigma) dr \quad (1)$$

Where $\epsilon_x^{LSDA}(\rho_\sigma) = -(3/4)(6/\pi)^{1/3}\rho_\sigma^{1/3}$ is the σ component of LSDA exchanges energy per particle, and $F_x(\rho_\sigma, \nabla\rho_\sigma, \tau_\sigma)$ is a relatively complementary complementary factor with one value for the uniform density. The correlation part of TPSS is not separated into spin-up and spin-down components in equation 2.

$$E_c^{TPSS}[\rho_\alpha, \rho_\beta] = \int \rho \epsilon_c^{revPKZB}\left[1 + d\left(\frac{\tau_w}{\tau}\right)^3 \epsilon_c^{revPKZB}\right] dr \quad (2)$$

Here $\rho = \rho_\alpha + \rho_\beta$, $\tau = \tau_\alpha + \tau_\beta$, $\tau_w = |\nabla_\rho|^2/8\rho$ $\epsilon_c^{revPKZB}(\rho_\alpha, \rho_\beta, \nabla\rho_\alpha, \nabla\rho_\beta, \tau)$ is the revised PKZB correlation energy per particle, and d is a nonempirical constant. The globally hybrid form of the MGGA functional is obtained by combination between TPSS with exact exchange in equation 3.

$$E_{xc}^{TPSSh} = aE_x^{exact} + (1-a)E_x^{TPSS} + E_c^{TPSS} \quad (3)$$

The TPSSh functional has an empiric parameter with optimal value as a = 0.1 was determined by minimizing the absolute deviation enthalpy of the 223 G3/99 molecules using the 6-311++G (3f,3pd) basis set.

Discussion about TPSS's meta-GGA in adiabatically hybrid version (one parameter) and the Perdew, Burke, and Ernzerhof's (PBEs) GGA adiabatics for determining excited energy. The calculation products showed that TPSS and TPSSh methods provide a product of exited energy fitted with experimental product, and develop a local adiabatic spin density approach, especially in adiabatic PBE GGA[14]. Based on computational results to determine atomic and molecular properties by comparing it with the experimental results. For atomic property, it is obtained that energy from spherical atom and ion demonstrated that TPSS's meta-GGA is more accurate compared with LSD, PBE GAA, and PKZB's meta-GGA. Meanwhile, the molecular properties determination showed that atomization energy and bond length are paid more properties attention in examining a new method in quantum chemistry[15]. The study of computational with TPSSh methods give result better accuracy. The theoretical NMR study for cation- π interactions in ethylenic complexes[16]. High-level ab initio calculations on the NiO_2 system[17]. Calculations Mössbauer and electrochemical investigation of ferrocenyltelluride derivatives[18]. Determination for atomization energies of molecules and surface energies of solid[15]. Determination energies to all electrons and reasonable spin-transition temperature[19]. The computational study for complexes of iron(II) with various ligand which transition spin characteristic have been conducted by previous research's[20,21,22,23].

3. Methodology

The determination from various character of complex coming from the transition metal requires for computational methods that involve electronic correlation effect. The investigative products on 20 types of molecule showed that TPSS's meta-GGA has a similar accuracy with the PKZB's meta-GGA in determining of atomization energy from a specific molecule and has a far better accuracy level in determination of bond length compared with the PKZB's meta-GGA[15]. Computational calculation used DFT, TPSSh function and TZVP basis set. The software used consists of the Gaussian 09, Revision D.01 (Frisch et al., 2013)[24] and Jmol see its visual output. The data get from product computational with Gaussian software is used to determine the stability complex as thermo chemistry data[25].

In a computational study, the compound structure data as bond length and bond angle is require used as input data. The structure data of the 1,2,4-4H-triazole–iron(II) complex has not been successfully determined, thus calculate computational used structure data the 1,2,4-4H-triazole – cooper(II) complex. Study structure of single crystal for $[Cu(hyetrz)_3](ClO_4)_2 3H_2O$ (hyetrz) 4-(2-hydroxyethyl)- 1,2,4-4H-triazole) complex used X-ray analysis. The product of study in the meanwhile connecting inter Cu(II) ions by triply bridges N1,N2-1,2,4-4H-triazole with distance inter Cu1-Cu2 is 3,853Å and Cu2-Cu3 is 3,829Å[26]. Study of SEM and X-ray powder diffraction for the $[Fe(NH_2trz)_3](NO_3)_2$ and $[Cu(NH_2trz)_3](NO_3)_2.H_2O$ complexes show that the both complexes have similarity of crystal structure[10].

In this study, there are two focus, they are determination of complex structure and determination of complex stability. A brief description about it would be explored as followings:

3.1. Prediction of complex structure

The determining of complexes structure with optimization are obtained bond length and bond angle data in Fe(II) 1,2,4-4H-triazole complex. In this study, the investigated complexes are the complexes of $[Fe_4(Htrz)_8(trz)_4]^{4+}$ and of $[Fe_4(Htrz)_{12}]^{8+}$.

3.2 Determination of complex stability

The stability of complex measured based on stability energy obtain at bond forming between iron(II) ion and the ligand in the oligomer form. $E_{stability} = E_{oligomer} - (E_{Fe\text{-}ion} + E_{ligand})$. The complex compound in which one of its ligand is deprotonated has the formula as the $[Fe_4(Htrz)_8(trz)_4]^{4+}$. Meanwhile another complex as a complex compounds in which its ligand is undeprotonated has the formula $[Fe_4(Htrz)_{12}]^{8+}$.

4. Result

4.1 Determination of Complex Structure

The computational jobs were geometry optimization for determining structure of complex compounds of $[Fe_4(Htrz)_{12}]^{8+}$ and $[Fe_4(Htrz)_8(trz)_4]^{4+}$, which are carried out by using the DFT with TPSSh method, and the TZVP basis set. The complex structure resulted from geometry optimization of $[Fe_4(Htrz)_{12}]^{8+}$ and $[Fe_4(Htrz)_8(trz)_4]^{4+}$ are presented in Figure. 2.

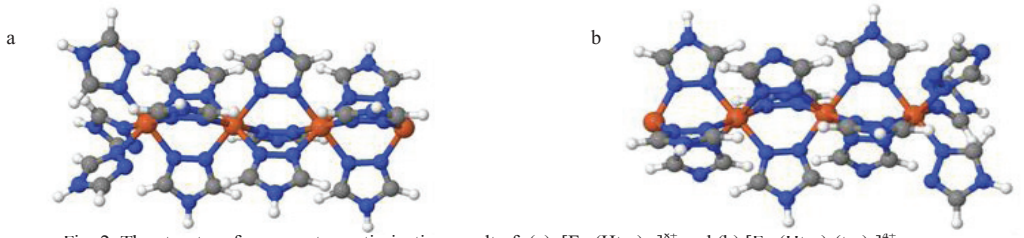

Fig. 2. The structure for geometry optimization result of: (a) $[Fe_4(Htrz)_{12}]^{8+}$ and (b) $[Fe_4(Htrz)_8(trz)_4]^{4+}$

The results of geometry optimization present some bond length and bond angle of the $[Fe_4(Htrz)_{12}]^{8+}$ and $[Fe_4(Htrz)_8(trz)_4]^{4+}$ complexes are presented in Table1 and 2.

Table 1.The bond length (Å) and angle of bond (degrees) for the complex of $[Fe_4(Htrz)_{12}]^{8+}$

The Bond	The bond length (Å)
Fe1 – Fe2	3.61
Fe2 – Fe3	3.84
Fe3 – Fe4	3.79
Fe2 – N7	2.04
N7 – C15	1.32
C15 – N22	1.35
N22 – C16	1.35
C16 – N8	1.32
N8 – Fe3	2.03
Fe3 – N73	2.04
Fe3 – N9	2.04
N73 – N74	1.39
C16 – H30	1.08

The Bond	The bond angle (degree)
N6 – Fe2 – N38	88.0
N72 – Fe3 – N9	92.1
N40 – Fe3 – N42	179.6
N38 – Fe2 – N39	179.9
N10 – Fe4 – N75	89.0
C47 – N54 – C48	106.5
C49 – N55 – C50	106.4
C79 – N71 – N72	106.8
C82 – N74 – N73	107.3
C79 – N71 – Fe2	127.2
C81 – N73 – Fe3	128.0
N71 – C79 – N86	109.9
N73 – C81 – N87	109.7

Table 2. The bond length (Å) and bond angle (degrees) for the complex of $[Fe_4(Htrz)_8(trz)_4]^{4+}$

The Bond	The bond length (Å)
Fe1 – Fe2	3.48
Fe2 – Fe3	3.69
Fe3 – Fe4	3.68
Fe2 – N70	2.00
Fe2 – N71	1.98
Fe2 – N7	1.99
Fe3 – N40	1.97
N71 – N72	1.38
N71 – C79	1.35
C79 – N86	1.33
C79 – H91	1.08
N86 – C80	1.34
N22 – H29	1.01

The Bond	The bond angle (degree)
N6 – Fe2 – N38	89.1
N72 – Fe3 – N9	91.8
N40 – Fe3 – N42	178.4
N38 – Fe2 – N39	179.9
N10 – Fe4 – N75	86.0
C47 – N54 – C48	106.6
C49 – N55 – C50	106.4
C79 – N71 – N72	105.2
C82 – N74 – N73	105.4
C79 – N71 – Fe2	128.7
C81 – N73 – Fe3	127.4
N71 – C79 – N86	113.7
N73 – C81 – N87	113.6

4.2 Determination of complex stability

The result of computational using the Gaussian 09 [24], they are obtained the energy of Fe(II) ion, Htrz, trz^{-1}, undeprotonated complexes and deprotonated complexes. Through such data utilization, it is determined the amount of energy differences in that complex formation. The result for computational data and the energy differences of the $[Fe_4(Htrz)_8(trz)_4]^{4+}$ and $[Fe_4(Htrz)_{12}]^{8+}$ complexes using several level of theory and basis set are presented in Table 3.

Table 3. The Computational result for the $[Fe_4(Htrz)_8(trz)_4]^{4+}$ and $[Fe_4(Htrz)_{12}]^{8+}$ complexes using several level of theory and basis set.

Level of theory and basis set	Complexes	Energy (Ht)				Energy difference (Ht)	Energy difference (kJ/mol)
		Fe	Htrz	trz	Complexes		
UHF/ 3-21G	$[Fe_4(Htrz)_8(trz)_4]^{4+}$	-1255.375	-239.358	-238.787	-7894.954	-3.440	-9030.415
	$[Fe_4(Htrz)_{12}]^{8+}$	-1255.375	-239.358		-7895.072	-1.274	-3345.602
UHF/ 6-31G(d)	$[Fe_4(Htrz)_8(trz)_4]^{4+}$	-1261.299	-240.728	-240.174	-7934.798	-3.076	-8075.981
	$[Fe_4(Htrz)_{12}]^{8+}$	-1261.299	-240.728		-7934.863	-0.924	-2426.552
B3LYP/ 3-21 G	$[Fe_4(Htrz)_8(trz)_4]^{4+}$	-1256.563	-240.823	-240.255	-7917.901	-4.046	-10621.834
	$[Fe_4(Htrz)_{12}]^{8+}$	-1256.563	-240.823		-7917.906	-1.781	-4675.720
B3LYP/ 6-31 G(d)	$[Fe_4(Htrz)_8(trz)_4]^{4+}$	-1262.447	-242.179	-241.530	-7957.537	-4.195	-11013.188
	$[Fe_4(Htrz)_{12}]^{8+}$	-1262.447	-242.179		-7957.518	-1.580	-4147.402
TPSSh/ TZVP	$[Fe_4(Htrz)_8(trz)_4]^{4+}$	-1262.646	-242.274	-241.731	-7959.243	-3.537	-9285.974
	$[Fe_4(Htrz)_{12}]^{8+}$	-1262.646	-242.274		-7959.212	-1.334	-3501.534

5. Discussion

5.1 Prediction of complex structure

The structure of $[Fe_4(Htrz)_8(trz)_4]^{4+}$ and $[Fe_4(Htrz)_{12}]^{8+}$ complexes from geometry optimization result are compared with the crystallography data for the $[Cu(NH_2trz)_3](NO_3)_2.H_2O$ complex result experimental measurement (Dirtu et al., 2010), the data result measurement EXAFS from $[Fe(Htrz)_2(trz)](BF_4)$ and $[Fe(Htrz)_3](BF_4)_2.H_2O$ complexes[27]. Based on comparison of bond length and bond angle for the Cu(II) 1,2,4-4H-triazole complex for measurement the experimental result with the geometry optimization result by the computational has a similarity, so that it is predicted that Fe(II) H-triazole polymeric structure is similar with the Cu(II) H-triazole polymer structure illustrated in Figure. 1. The detail comparison structure data result geometry optimization with experimental data proposed comparison bond length and bond angle. The result geometry optimization of distance between Fe(II) ion is 3.48Å - 3.68Å. Meanwhile, based measurement EXAFS distance between Fe(II) ion is 3.65Å[27]. The result geometry optimization of bond length Fe–N is 1.97Å - 2.00Å. Meanwhile, experimental result bond length for Cu(II) complex is 1.991Å - 2.372Å[10] and bond length for Cu(II) complex is 1.996Å - 2.381Å[26]. The result geometry optimization of bond length N–N is 1,38Å. Meanwhile, the experimental result bond length for Cu(II) complex is 1.385Å - 1.402Å (Dirtu et al., 2010). The result geometry optimization of bond length C–N is 1.34Å - 1.35Å. Meanwhile, the experimental result bond length for Cu(II) complex is 1.300Å - 1.344Å (Dirtu et al., 2010).

The axial position, the result of geometry optimization bond angle N–Fe–N for Fe(II) complex is 178.4° – 179.9°. Meanwhile, the experimental result bond angle N–Cu–N for Cu(II) complex is 180.0° [10], and the other

experimental result bond angle N–Cu–N for Cu(II) complex is 171.7° – 180.0° [26]. In equatorial position, the result of geometry optimization bond angle N–Fe–N for Fe(II) complex is 86.0° – 92.1°. Meanwhile, the experimental result bond angle N–Cu–N for Cu(II) complex is 87.10° – 92.60° and the other experimental result bond angle N–Cu–N for Cu(II) complex is 86.3° – 95.5° [26]. The result of geometry optimization bond angle C–N–C for Fe(II) complex is 106.4° – 106.6°. Meanwhile, the experimental result bond angle C–N–C for Cu(II) complex is 105.5° [10]. The result of geometry optimization bond angle C–N–N for Fe(II) complex is 105.2°–107.3°. Meanwhile, the experimental result bond angle C–N–N for Cu(II) complex is 106.7° – 107.0° [10]. The result of geometry optimization bond angle C-N–Fe for Fe(II) complex is 127.2° – 128.7°. Meanwhile, the experimental result bond angle C-N–Cu for Cu(II) complex is 128.10° [10], and and the other experimental result bond angle C-N–Cu for Cu(II) complex is 123.7° – 131.6° [26]. The result of geometry optimization bond angle N–C–N for Fe(II) complex is 109.7° – 113.7°. Meanwhile, the experimental result bond angle N–C–N for Cu(II) complex is 110.2° – 111.2° [10].

5.2 Determination of complex stability

Based on energy difference data presented in Table 3 used to compare energy differences between the $[Fe_4(Htrz)_8(trz)_4]^{4+}$ and $[Fe_4(Htrz)_{12}]^{8+}$ complexes using several level of theory and basis set as it is illustrated in Figure 3.

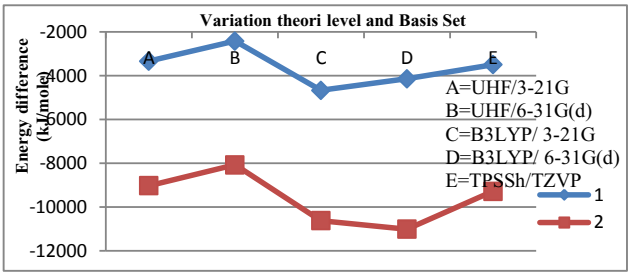

Fig. 3. The curve of energy difference for the $[Fe_4(Htrz)_8(trz)_4]^{4+}$ and $[Fe_4(Htrz)_{12}]^{8+}$ complexes using several level of theory and basis set. where: (1) is data of the $[Fe_4(Htrz)_{12}]^{8+}$ complex and (2) is data of the $[Fe_4(Htrz)_8(trz)_4]^{4+}$ complex.

The curve of energy difference for the $[Fe_4(Htrz)_8(trz)_4]^{4+}$ and $[Fe_4(Htrz)_{12}]^{8+}$ complexes using several level of theory and basis set as illustrated in Figure. 3 showed that comparison between $[Fe_4(Htrz)_8(trz)_4]^{4+}$ complex is more stable compared to the $[Fe_4(Htrz)_{12}]^{8+}$ complexes. The comparison between those two complexes is consistent for all computational results using several level of theory and basis set.

Conclusions

Based on computational results, the predicted structure of $[Fe_4(Htrz)_8(trz)_4]^{4+}$ and $[Fe_4(Htrz)_{12}]^{8+}$ polymeric complexes were modeled. The energy difference using DFT, TPSSh method, and TZVP basis set for $[Fe_4(Htrz)_8(trz)_4]^{4+}$ complex was -9285,974 kJ/mole and for $[Fe_4(Htrz)_{12}]^{8+}$ complex was -3501,534 kJ/mole. The relative stability of the complexes showed consistent results computationally with lower level theory of HF and DFT with 3-21G and 6-31G (d) basis set. The deprotonated complexes of iron(II) 1,2,4-triazole are more stable than the protonated ones, $[Fe_4(Htrz)_8(trz)_4]^{4+}$ complex was more stable than $[Fe_4(Htrz)_{12}]^{8+}$ complex.

References

1. Reger, D.L., Gardinier, J.R., Smith, M.D., Shahin, A.M., Long, G.J., Rebbouh, L., Grandjean, F.,. Polymorphism in Fe[(p-IC6H4)B(3-Mepz)3]2 (pz = Pyrazolyl): Impact of Supramolecular Structure on an Iron(II) Electronic Spin-State Crossover. *Inorg. Chem.* 2005; 44, 1852–1866. doi:10.1021/ic048406q.
2. Wu, C.-C., Jung, J., Gantzel, P.K., Gütlich, P., Hendrickson, D.N.,. LIESST Effect Studies of Iron(II) Spin-Crossover Complexes with Phosphine Ligands: Relaxation Kinetics and Effects of Solvent Molecules. *Inorg. Chem.* 1997; 36, 5339–5347. doi:10.1021/ic9700359
3. Herchel, R., Boča, R., Gembický, M., Kožíšek, J., Renz, F., Spin Crossover in a Tetranuclear Cr(III)−Fe(III)3 Complex. *Inorg. Chem.* 2004; 43, 4103–4105. doi:10.1021/ic035374i

4. Piquer, C., Grandjean, F., Mathon, O., Pascarelli, S., Reger, D.L., Little, C.A., Long, G.J.,. A High-Pressure Iron K-Edge X-ray Absorption Spectral Study of the Spin-State Crossover in {Fe[HC(3,5-(CH3)2pz)3]2}I2 and {Fe[HC(3,5-(CH3)2pz)3]2}(BF4)2. *Inorg. Chem*. 2003; 42, 982–985. doi:10.1021/ic0204530.
5. Létard, J.-F., Guionneau, P., Goux-Capes, L., *Towards Spin Crossover Applications, in: Spin Crossover in Transition Metal Compounds III, Topics in Current Chemistry*. Springer Berlin Heidelberg, 2004; pp. 221–249.
6. Kahn, O., Martinez, C.J.,. Spin-Transition Polymers: From Molecular Materials Toward Memory Devices. *Science* 279, 44–48. doi:10.1126/*science*. 1998; 279.5347.44
7. Sugiyarto, K., Goodwin, H.,. Cooperative Spin Transitions in Iron(II) Derivatives of 1,2,4-Triazole. *Aust. J. Chem*. 1994; 47, 263–277.
8. Faulmann, C., Chahine, J., Malfant, I., Caro, D. de, Cormary, B., Valade, L., A facile route for the preparation of nanoparticles of the spin-crossover complex [Fe(Htrz)2(trz)](BF4) in xerogel transparent composite films. *Dalton Trans*. 2011; 40, 2480–2485. doi:10.1039/C0DT01586E
9. Lavrenova, L.G., Shakirova, O.G., Ikorskii, V.N., Varnek, V.A., Sheludyakova, L.A., Larionov, S.V.,. 1 A 1 ⇄ 5 T 2 Spin Transition in New Thermochromic Iron(II) Complexes with 1,2,4-Triazole and 4-Amino-1,2,4-Triazole. *Russian Journal of Coordination Chemistry* 2003; 29, 22–27. doi:10.1023/A:1021834715674
10. Dîrtu, M.M., Neuhausen, C., Naik, A.D., Rotaru, A., Spinu, L., Garcia, Y., Insights into the Origin of Cooperative Effects in the Spin Transition of [Fe(NH2trz)3](NO3)2: the Role of Supramolecular Interactions Evidenced in the Crystal Structure of [Cu(NH2trz)3](NO3)2•H2O. *Inorg. Chem*. 2010; 49, 5723–5736. doi:10.1021/ic100667f
11. Urakawa, A., Van Beek, W., Monrabal-Capilla, M., Galán-Mascarós, J.R., Palin, L., Milanesio, M.,. Combined, Modulation Enhanced X-ray Powder Diffraction and Raman Spectroscopic Study of Structural Transitions in the Spin Crossover Material [Fe(Htrz)2(trz)](BF4). *J. Phys. Chem.* C 2011; 115, 1323–1329. doi:10.1021/jp107206n.
12. Cohen, A.J., Mori-Sánchez, P., Yang, W., Challenges for Density Functional Theory. *Chem. Rev*. 2012; 112, 289–320. doi:10.1021/cr200107z
13. Staroverov, V.N., Scuseria, G.E., Tao, J., Perdew, J.P.,. Comparative assessment of a new nonempirical density functional: Molecules and hydrogen-bonded complexes. *The Journal of Chemical Physics* 2003; 119, 12129–12137. doi:10.1063/1.1626543
14. Tao, J., Tretiak, S., Zhu, J.-X.,. Performance of a non-empirical meta-GGA density functional for excitation energies. *The Journal of Chemical Physics* 2008; 128, 084110. doi:10.1063/1.2837831
15. Perdew, J.P., Ruzsinszky, A., Tao, J., Staroverov, V.N., Scuseria, G.E., Csonka, G.I., Prescription for the design and selection of density functional approximations: More constraint satisfaction with fewer fits. *The Journal of Chemical Physics* 2005; 123, 062201. doi:10.1063/1.1904565.
16. Ebrahimi, A., Khorassani, M.H., Masoodi, H.R.,. The role of cation–π interactions in ethylenic complexes: A theoretical NMR study. *Chemical Physics Letters*. 2010; 493, 27–32. doi:10.1016/j.cplett.2010.04.064
17. Song, J., Aprá, E., Khait, Y.G., Hoffmann, M.R., Kowalski, K.,. High-level ab initio calculations on the NiO2 system. *Chemical Physics Letters* 2006; 428, 277–282. doi:10.1016/j.cplett.2006.07.075
18. Torubaev, Y.V., Pasynskii, A.A., Pavlova, A.V., Tauqeer, M., Herber, R.H., Nowik, I., Skabitskii, I.V., Denisov, G.L., Grinberg, V.A., Mathur, P., Shaikh, M.M., Lahiri, G.K., Synthesis, molecular structures, Mössbauer and electrochemical investigation of ferrocenyltelluride derivatives: (Fc2Te2)Fe(CO)3I2 [(CO)3IFe(μ-TeFc)]2, CpFe(CO)2TeFc, CpFe(CO)2TeX2Fc (X = Br, I) and CpFe(CO)2(μ-TeFc)Fe(CO)3I2. *Journal of Organometallic Chemistry* 2015; 777, 88–95. doi:10.1016/j.jorganchem.2014.11.025
19. Kaneko, M., Tokinobu, S., Nakashima, S., Density Functional Study on Spin-crossover Phenomena of Assembled Complexes, [Fe(NCX)2(bpa)2]n (X = S, Se, and BH3; bpa: 1,2-bis(4-pyridyl)ethane). *Chemistry Letters* 2013; 42, 1432–1434. doi:10.1246/cl.130712
20. Zein, S., Matouzenko, G.S., Borshch, S.AQuantum Chemical Study of Three Polymorphs of the Mononuclear Spin-Transition Complex [Fe(DPPA)(NCS)2]. *J. Phys. Chem. A* ., 2005; 109, 8568–8571. doi:10.1021/jp051958p.
21. Güell, M., Luis, J.M., Solà, M., Swart, M., Importance of the Basis Set for the Spin-State Energetics of Iron Complexes. *J. Phys. Chem*. A 2008; 112, 6384–6391. doi:10.1021/jp803441m
22. Van Kuiken, B.E., Khalil, M.,. Simulating Picosecond Iron K-Edge X-ray Absorption Spectra by ab Initio Methods To Study Photoinduced Changes in the Electronic Structure of Fe(II) Spin Crossover Complexes. *J. Phys. Chem*. A 2011; 115, 10749–10761. doi:10.1021/jp2056333
23. Furukawa, S., Hitomi, Y., Shishido, T., Teramura, K., Tanaka, T.,. π Back-Bonding of Iron(II) Complexes Supported by Tris(pyrid-2-ylmethyl)amine and Its Nitro-Substituted Derivatives. *J. Phys. Chem. A* 2011; 115, 13589–13595. doi:10.1021/jp2069539
24. Frisch M. J., G. W. Trucks, H. B. Schlegel, G. E. Scuseria, M. A. Robb, J. R. Cheeseman, G. Scalmani, V. Barone, B. Mennucci, G. A. Petersson, H. Nakatsuji, M. Caricato, X. Li, H. P. Hratchian, A. F. Izmaylov, J. Bloino, G. Zheng, J. L. Sonnenberg, M. Hada, M. Ehara, K. Toyota, R. Fukuda, J. Hasegawa, M. Ishida, T. Nakajima, Y. Honda, O. Kitao, H. Nakai, T. Vreven, J. A. Montgomery, Jr., J. E. Peralta, F. Ogliaro, M. Bearpark, J. J. Heyd, E. Brothers, K. N. Kudin, V. N. Staroverov, T. Keith, R. Kobayashi, J. Normand, K. Raghavachari, A. Rendell, J. C. Burant, S. S. Iyengar, J. Tomasi, M. Cossi, N. Rega, J. M. Millam, M. Klene, J. E. Knox, J. B. Cross, V. Bakken, C. Adamo, J. Jaramillo, R. Gomperts, R. E. Stratmann, O. Yazyev, A. J. Austin, R. Cammi, C. Pomelli, J. W. Ochterski, R. L. Martin, K. Morokuma, V. G. Zakrzewski, G. A. Voth, P. Salvador, J. J. Dannenberg, S. Dapprich, A. D. Daniels, O. Farkas, J. B. Foresman, J. V. Ortiz, J. Cioslowski, and D. J. Fox, Gaussian, Inc., Wallingford CT, 2013.
25. Ochterski, Joseph W., *Thermochemistry in Gaussian*, (2000): help@gaussian.com
26. Garcia, Y., van Koningsbruggen, P.J., Bravic, G., Guionneau, P., Chasseau, D., Cascarano, G.L., Moscovici, J., Lambert, K., Michalowicz, A., Kahn, O., Synthesis, Crystal Structure, EXAFS, and Magnetic Properties of catena-Poly[μ-tris(4-(2-hydroxyethyl)-1,2,4-triazole-N1,N2)copper(II)] Diperchlorate Trihydrate: Relevance with the Structure of the Iron(II) 1,2,4-Triazole Spin Transition Molecular Materials. *Inorg. Chem*. 1997; 36, 6357–6365. doi:10.1021/ic970895p
27. Michalowicz, A., Moscovici, J., Ducourant, B., Cracco, D., Kahn, O., EXAFS and X-ray powder diffraction studies of the spin transition molecular materials [Fe(Htrz)2(trz)](BF4) and [Fe(Htrz)3](BF4)2.H2O (Htrz = 1,2,4-4H-triazole; trz = 1,2,4-triazolato). *Chem. Mater.* 1995; 7, 1833–1842. doi:10.1021/cm00058a013.